Carbon isotopic evidence for the associations of decreasing atmospheric CO_2 level with the Frasnian-Famennian mass extinction

Bing Xu,[1] Zhaoyan Gu,[1] Chengyuan Wang,[2] Qingzhen Hao,[1] Jingtai Han,[1] Qiang Liu,[1] Luo Wang,[1] and Yanwu Lu[1]

Received 30 August 2011; revised 13 December 2011; accepted 21 January 2012; published 16 March 2012.

[1] A perturbation of the global carbon cycle has often been used for interpreting the Frasnian-Famennian (F-F) mass extinction. However, the changes of atmospheric CO_2 level (pCO_2) during this interval are much debatable. To illustrate the carbon cycle during F-F transition, paired inorganic ($\delta^{13}C_{carb}$) and organic ($\delta^{13}C_{org}$) carbon isotope analyses were carried out on two late Devonian carbonate sequences (Dongcun and Yangdi) from south China. The larger amplitude shift of $\delta^{13}C_{org}$ compared to $\delta^{13}C_{carb}$ and its resultant $\Delta^{13}C$ ($\Delta^{13}C = \delta^{13}C_{carb} - \delta^{13}C_{org}$) decrease indicate decreased atmospheric CO_2 level around the F-F boundary. The onset of pCO_2 level decrease predates that of marine regressions, which coincide with the beginning of conodont extinctions, suggesting that temperature decrease induced by decreased greenhouse effect of atmospheric CO_2 might have contributed to the F-F mass extinction.

Citation: Xu, B., Z. Gu, C. Wang, Q. Hao, J. Han, Q. Liu, L. Wang, and Y. Lu (2012), Carbon isotopic evidence for the associations of decreasing atmospheric CO_2 level with the Frasnian-Famennian mass extinction, *J. Geophys. Res.*, *117*, G01032, doi:10.1029/2011JG001847.

1. Introduction

[2] The Frasnian-Famennian (F-F) mass extinction is one of the five big mass extinctions in the Phanerozoic, during which a significant reduction in biodiversities occurred, though the extinction extensity is not as large as those in end Ordovician, end Permian, and end Cretaceous [*Bambach et al.*, 2004; *Racki*, 2005; *Stigall*, 2010]. The cause of this bioevent remains a subject of intensive debate with both external (bolide impact) and internal (e.g., increased hydrothermal-volcanic activities, climate changes) mechanisms invoked [*McGhee*, 1996; *Racki*, 2005]. Most mechanisms are involved in a $\delta^{13}C_{carb}$ positive excursion around the F-F boundary [*McGhee*, 1996; *Joachimski et al.*, 2002; *Ma and Bai*, 2002; *Racki et al.*, 2002; *Goddéris and Joachimski*, 2004; *Riquier et al.*, 2006; *van Geldern et al.*, 2006; *Xu et al.*, 2008; *John et al.*, 2010; *Zeng et al.*, 2011]. The $\delta^{13}C_{carb}$ positive excursion, together with organic rich horizons known as the Upper Kellwasser horizons in biostratigraphy [*Schindler*, 1990; *Walliser*, 1996], is interpreted as the result of increased carbon burial [*McGhee et al.*, 1986; *Joachimski et al.*, 2002; *Ma and Bai*, 2002; *Racki et al.*, 2002; *Xu et al.*, 2008]. It is suggested that atmospheric CO_2 level would decease with increased organic carbon burial [*Kump and Arthur*, 1999], leading to climate change and thus mass extinction [*Joachimski et al.*, 2002; *Racki et al.*, 2002]. However, to our knowledge, no direct evidence supports a decrease of pCO_2 level around the F-F boundary, complicating the interpretation of the F-F mass extinction by the global carbon cycle change.

[3] $\Delta^{13}C$ is often used as reliable paleo-pCO_2 barometer [*Cramer and Saltzman*, 2007; *Young et al.*, 2008], because the isotopic difference between carbonate and organic matter is dominated by photosynthetic fractionation, which partly depends on the concentration of dissolved CO_2 in seawater [e.g., *Popp et al.*, 1989; *Freeman and Hayes*, 1992; *Hayes et al.*, 1999]. Unfortunately, most previous studies focused separately on the changes of inorganic and organic carbon isotope [*McGhee et al.*, 1986; *Joachimski and Buggisch*, 1993; *Wang et al.*, 1996; *Racki et al.*, 2002; *Xu et al.*, 2003; *Buggisch and Joachimski*, 2006; *Izokh et al.*, 2009], few examined the variations of $\Delta^{13}C$. Even the few $\Delta^{13}C$ data seem to change geographically [*Joachimski*, 1997; *Chen et al.*, 2005]. In the Baisha and Fuhe sections from south China, $\Delta^{13}C$ shows high-frequency vibrations around the F-F boundary [*Chen et al.*, 2005], but it is suggested that there is no obvious change in Europe [*Joachimski et al.*, 2002].

[4] In this study, high-resolution analyses of coupled inorganic and organic carbon isotope were carried out on two late Devonian carbonate sequences (Dongcun and Yangdi) in south China. The primary aims of this study are to characterize the changes of atmospheric CO_2 level during

[1]Key Laboratory of Cenozoic Geology and Environment, Institute of Geology and Geophysics, Chinese Academy of Sciences, Beijing, China.
[2]Nanjing Institute of Geology and Palaeontology, Chinese Academy of Sciences, Nanjing, China.

0148-0227/12/2011JG001847

the F-F transition and address the links between the perturbation of the global carbon cycle and the mass extinction.

2. Sampling and Methodology

[5] Dongcun section (N24.95°, E110.42°) is located at the Dongcun village, about 20 km northwest of Yangshuo (Figure 1). A total of 12 conodont zones from *transitants* to *crepida* are recognized [*Wang*, 1994; *Wang and Ziegler*, 2002]. The F-F (*triangularis*/*linguiformis*) boundary is located at 2.0 m above a thin dark micritic limestone from which most of conodonts of the *linguiformis* fauna disappeared [*Wang and Ziegler*, 2002]. The Yangdi section is situated to the northeast of the Dongcun section (Figure 1). The conodont zones of Yangdi section is identified by *Ji* [1994].

[6] Total 451 samples were collected in this study, 201 from Dongcun section and 250 from Yangdi section. Eighty-nine samples were selected for paired analysis of inorganic and organic carbon isotope (51 from Dongcun section, 38 from Yangdi section). Only $\delta^{13}C_{carb}$ was analyzed for the rest samples. All specimens were cleaned by ultrasonication and dried under room temperature. Micritic components were preferentially sampled for carbon isotope analysis because of their little diagenetic alteration [*Marshall*, 1992]. For the specimens with limited micritic components (marlstone and grainstone), the nonrecrystallized or insignificantly recrystallized parts were sampled by drilling under microscope. The sample powders were reacted with 100% phosphoric acid for 12 h under 50°C. The produced CO_2 was collected with liquid nitrogen, and isotopic ratios of $^{13}C/^{12}C$ were measured by MAT 252 mass spectrometer. For organic carbon isotope analysis, 50–100 g sample powder reacted with 1 M HCl for removing carbonate. The HCl-insoluble residues of samples were combusted offline, and the evolved CO_2 gas was submitted to mass spectrometric measurement. The isotopic data were reported in the conventional δ notation as per mil (‰) deviation relative to the PDB standard. The precision measured by multianalysis of both GBW04405 (National stable isotope of carbon and oxygen in carbonate) and replicate samples is better than 0.1‰ for carbon isotope.

3. Results

[7] In both Dongcun and Yangdi sections, $\delta^{13}C_{carb}$ exhibits an increasing pattern from Frasnian to Famennian with two peaks in the late *rhenana* zone and around the F-F boundary (Figure 2). These two positive excursions are comparable with the records from other continents including Europe, America, and Africa [*McGhee et al.*, 1986; *Joachimski and Buggisch*, 1993; *Joachimski*, 1997; *Joachimski et al.*, 2002; *Wang et al.*, 1996; *Buggisch and Joachimski*, 2006], and correspond to the two Kellwasser horizons in biostratigraphy [*Xu et al.*, 2008]. Detailed observation shows that the $\delta^{13}C_{carb}$ excursion that occurred around the F-F boundary is composed of two-stepwise increases (Figure 2). In Dongcun section, $\delta^{13}C_{carb}$, first increases from 0.8‰ to 1.5‰ during the interval of 2.4–1.9 m below the F-F boundary, and then remains a relative stable value before it increases again at the F-F boundary (Figure 2).

[8] The $\delta^{13}C_{org}$ parallels $\delta^{13}C_{carb}$ along the profiles of the Dongcun and Yangdi sections, and also shifts to positive in the late *rhenana* zone and around the F-F boundary (Figure 2). Noteworthily, the amplitudes of the $\delta^{13}C_{org}$ excursions are larger than those of $\delta^{13}C_{carb}$ shifts (Table 1). At the F-F boundary, $\delta^{13}C_{org}$ has an increase of 4.0‰ and 4.5‰ in the Dongcun and Yangdi sections, respectively, while their corresponding shifts of $\delta^{13}C_{carb}$ are less than 3.0‰ (Figure 2). In the *rhenana* zone, the excursions of $\delta^{13}C_{carb}$ are smaller than 2.0‰ in both sections, but the shifts of $\delta^{13}C_{org}$ are individually more than 4.0‰ in the Dongcun section and 3.5‰ in the Yangdi section (Figure 2).

4. Discussion

4.1. Perturbations of the Global Carbon Cycle

[9] Although the carbon isotopic signatures of carbonate might be altered during diagenetic processes, it is safe to assume that the $\delta^{13}C_{carb}$ of our samples should mainly reflect the original signals. First, the carbon isotope compositions of micritic carbonate are regarded as being resistant to diagenetic influence [*Marshall*, 1992; *Rosales et al.*, 2001; *Saltzman*, 2002; *Joachimski et al.*, 2002; *Buggisch and Joachimski*, 2006]. Second, alterations of original $\delta^{13}C_{carb}$ signatures usually occur in the rocks containing soil organic matter [*Allan and Matthews*, 1982; *Lohmann*, 1988], or in organic carbon rich sediments, such as black shale [*Joachimski et al.*, 2002; *Buggisch and Joachimski*, 2006]. In both cases, $\delta^{13}C_{carb}$ would shift to low values because the CO_2 derived from these sources is ^{13}C depleted. The absence of organic rich or shaly horizons in both the Dongcun and Yangdi sections suggests fewer alterations of carbon isotope composition. Third, except for methanogenesis, no diagenetic process is known to result in an enrichment of ^{13}C during recrystallization [*Buggisch and Joachimski* 2006]. Therefore, in most cases, the positive excursions in $\delta^{13}C$ of carbonate rocks are representative of the original signatures. Finally, the comparable isotope pattern observed in the Dongcun and Yangdi sections, which are deposited under different environmental conditions, also supports little alteration of primary signals [*Buggisch and Joachimski*, 2006].

[10] For the organic carbon isotope, the respiratory remineralization of organic matter in sediment column under oxic condition can produce an enrichment in ^{13}C. This enrichment increases in sediments deposited beneath an anoxic water column [*Hayes et al.*, 1989; *Gong and Hollander*, 1997; *Fischer et al.*, 1998], where it can reach as high as 3‰. In the Dongcun and Yangdi sections, $\delta^{13}C_{org}$ shows an increasing pattern with the decrease of oxygenation level at the beginning, but it still increases after the water mass return to oxic condition [*Xu et al.*, 2008], indicating respiration of organic matter could not be the controlling factor for the $\delta^{13}C_{org}$ shifts.

[11] An obvious decrease in $\Delta^{13}C$ occurs near the F-F boundary in both the Dongcun and Yangdi sections due to a larger amplitude shift of $\delta^{13}C_{org}$ than $\delta^{13}C_{carb}$ (Figure 3). This differs from the previous observations on other sections [*Joachimski et al.*, 2002; *Chen et al.*, 2005]. Early paired analysis on the Berner section showed that the onset of $\delta^{13}C_{org}$ excursion predated that of $\delta^{13}C_{carb}$ around the F-F

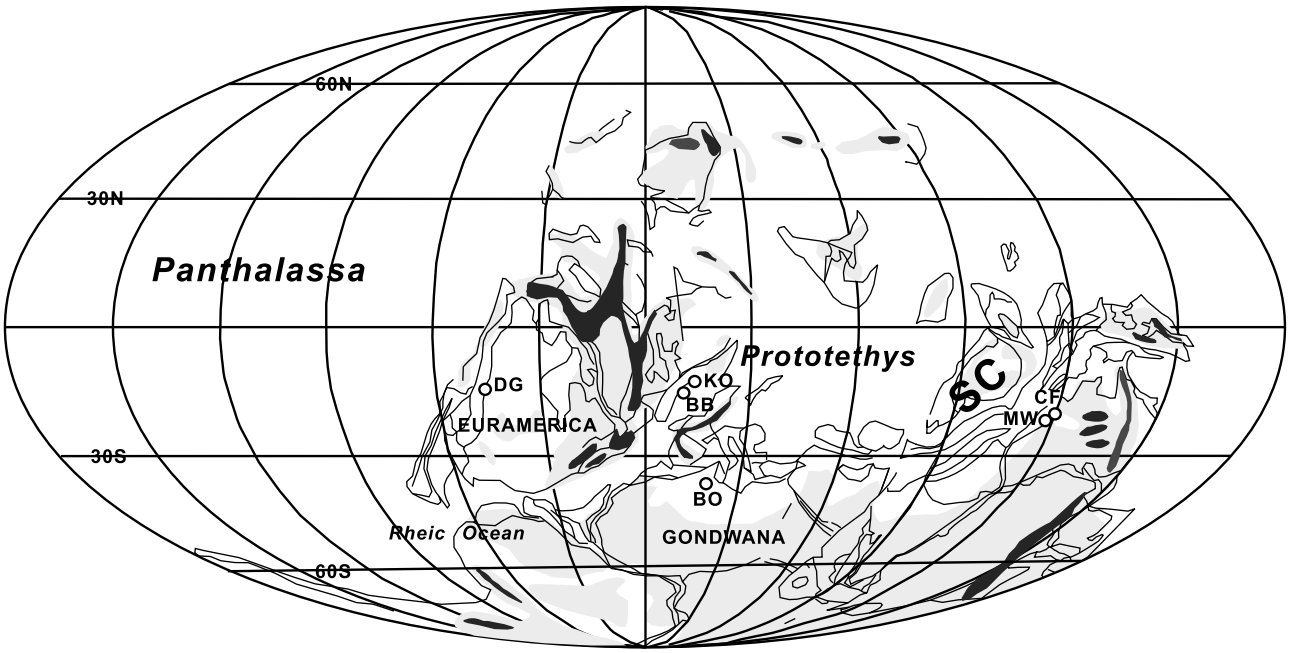

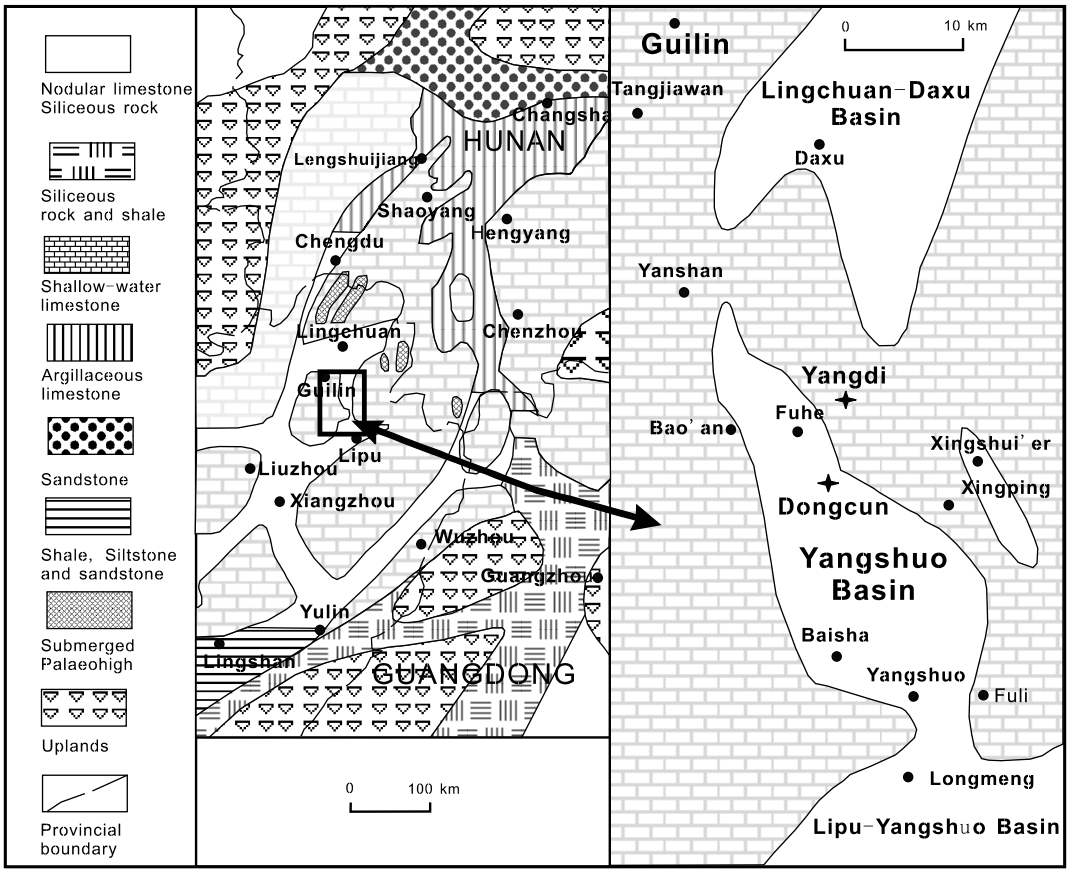

Figure 1. Paleogeographic location of south China (SC) [*Joachimski et al.*, 2002] and depositional context of the Dongcun and Yangdi sections.

boundary [*Joachimski*, 1997]. The later organic carbon isotope analyses on the Kowala section showed that the $\delta^{13}C_{org}$ displayed similar amplitude excursion with the $\delta^{13}C_{carb}$ shifts measured in other sections [*Joachimski et al.*, 2002]. Based on the above evidence, *Joachimski et al.* [2002] proposed that the high atmospheric and oceanic CO_2 concentrations of the Devonian resulted in the maximum photosynthetic fractionation, and thus any change in CO_2

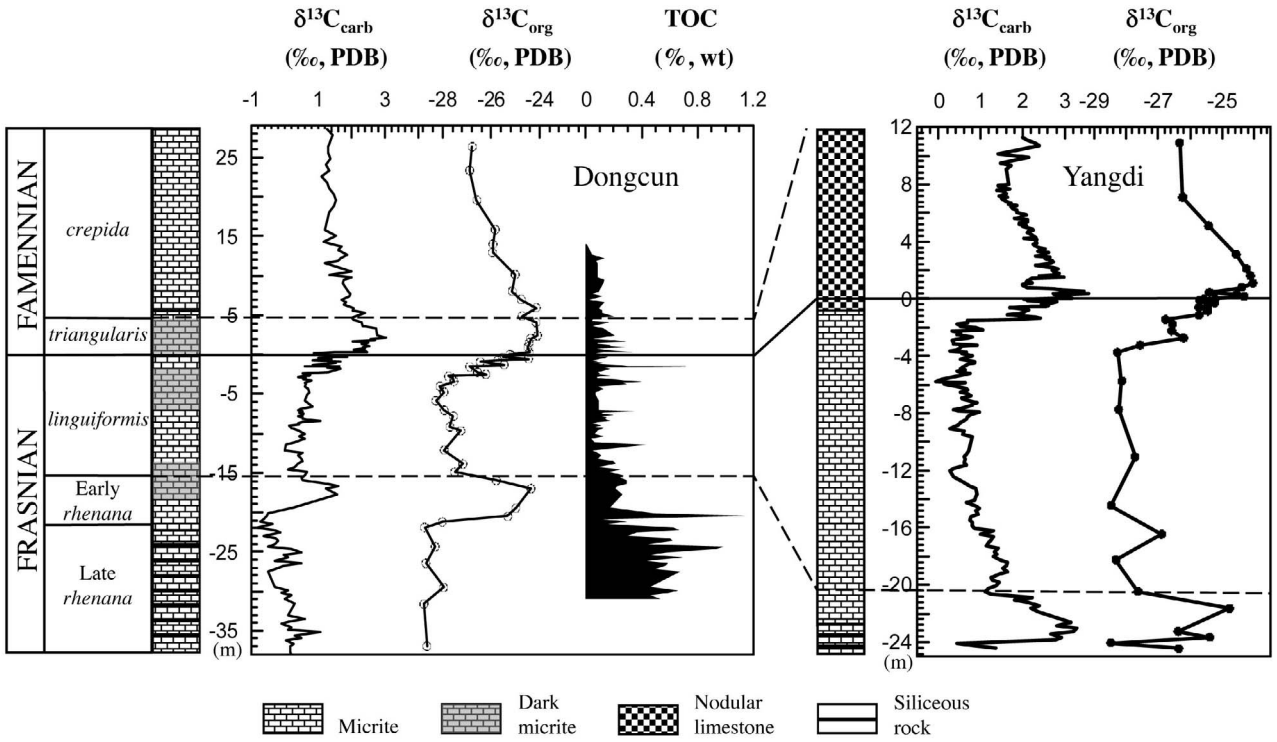

Figure 2. Distributions of $\delta^{13}C_{carb}$ and $\delta^{13}C_{org}$ along the sequences of the Dongcun and Yangdi sections ($\delta^{13}C_{carb}$ data adopted from *Xu et al.* [2008]).

concentration would not affect isotope fractionation during photosynthesis. However, the obvious $\Delta^{13}C$ excursion, together with larger amplitude shift of $\delta^{13}C_{org}$ than $\delta^{13}C_{carb}$ measured in the end Ordovician [*Young et al.*, 2008] and Early Silurian [*Cramer and Saltzman*, 2007] suggested that photosynthetic fractionation might not reach maximum in the late Devonian, because the atmospheric CO_2 levels of the former are much higher than the latter [*Banner and Hanson*, 1990; *Berner and Kothavala*, 2001]. Furthermore, the conclusion of *Joachimski et al.* [2002] relies on an assumption that the carbon isotope records from different regions reflect a global carbon cycle change. This assumption, however, is potentially flawed, because the carbon isotope composition of dissolved carbon and organic matter is controlled not only by global but also by local carbon cycle [*Panchuk et al.*, 2006]. Factors controlling local carbon cycle, such as circulation patterns, changes in primary productivity and phytoplankton community, can lead to carbon isotope variations [*Freeman and Hayes*, 1992; *Laws et al.*, 1997; *Bidigare et al.*, 1997; *Popp et al.*, 1989; *Hayes et al.*, 1999; *Des Marais*, 2001; *Panchuk et al.*, 2006]. Circulation patterns influence the exchange rates of dissolved inorganic carbon between water mass, particularly in regions of epeiric seas [*Panchuk et al.*, 2006]. Different species of phytoplankton, even the same species with different growth rate, might have different photosynthetic fractionations [*Freeman and Hayes*, 1992; *Francois et al.*, 1993; *Laws et al.*, 1997; *Bidigare et al.*, 1997; *Popp et al.*, 1989; *Hayes et al.*, 1999], causing variations of $\delta^{13}C_{org}$. As a result, the values and patterns of carbon isotope compositions might be different among various regions due to the difference in signal strength of the regional carbon cycle. This point is supported by the inconsistence in the amplitude of $\delta^{13}C_{carb}$ shifts around the F-F boundary measured in different regions. For example, at the Cinquefoil Mountain section, Alberta, Canada [*Wang et al.*, 1996], the excursion is from 1‰ to 5‰, whereas it is about 3‰ in some sections from Europe [*Joachimski et al.*, 2002]. In addition, there is a potential for partial alteration of original isotope signals during deposition and diagenetic processes. For these reasons, it is more reasonable to use the whole trend of the difference between $\delta^{13}C_{carb}$ and $\delta^{13}C_{org}$ of the same stratum to decipher the carbon cycle change [*Cramer and Saltzman*, 2007], and the consistent pattern of carbon isotope records from various sections should have a global significance. In the Kowala section, amplitude of the $\delta^{13}C_{org}$ excursion around the F-F boundary is not only larger than the $\delta^{13}C_{carb}$, but also larger than the difference between the maximum and minimum values of $\delta^{13}C_{carb}$ for all samples [*Joachimski et al.*, 2002]. Furthermore, the $\delta^{13}C_{carb}$ shifts recorded in the Plucki, Psie Górki, and Dębnik sections (around or less than +2‰), which are located in the same area with the Kowala section (around Kielce), are also less than the $\delta^{13}C_{org}$ excursion recorded in the Kowala section [*Racki et al.*, 2002]. Therefore, the carbon isotope records from Poland also support a decrease in $\Delta^{13}C$ around the F-F boundary, and indicate that the photosynthetic fractionation might not reach maximum in the late Devonian.

[12] In the Baisha and Fuhe sections, $\Delta^{13}C$ displays high-frequency vibrations across the F-F boundary [*Chen et al.*, 2005]. However, this pattern of $\Delta^{13}C$ is caused by several negative shifts of $\delta^{13}C_{carb}$. As suggested by *Buggisch and Joachimski* [2006], the lower values observed during the increase of $\delta^{13}C_{carb}$ are usually diagenetic signatures. In

Table 1. Carbon Isotope Data of the Dongcun and Yangdi Sections

Code	Depth	$\delta^{13}C_{carb}$	$\delta^{13}C_{org}$	$\Delta^{13}C$	Fossil Age	Code	Depth	$\delta^{13}C_{carb}$	$\delta^{13}C_{org}$	$\Delta^{13}C$	Fossil Age
					Dongcun Section						
DC435	28.58	1.26				DC409	11.88	1.61			
DC434	27.83	1.43				DC408	11.53	1.21			
DC432	26.33	1.30	−26.78	28.08		DC405	10.48	2.01			
DC431	25.58	1.29				DC404	10.13	1.33	−25.01	26.34	
DC430	24.83	1.37				DC403	9.78	2.01			
DC429	24.08	1.25				DC402	9.43	1.77			
DC428	23.33	1.33	−26.89	28.22		DC401	9.08	1.73			
DC427	22.58	1.09				DC398	8.03	1.89	−25.13	27.02	
DC426	21.83	1.28				DC397	7.68	1.97			
DC425	21.08	1.33				DC396	7.33	1.93			
DC424	20.33	1.48				DC395	6.98	1.71	−24.76	26.47	
DC423	19.58	1.54	−26.59	28.13		DC394	6.63	1.83			
DC422	18.83	1.46				DC393	6.28	1.77			
DC421	18.08	1.34				DC392	5.93	2.07	−24.14	26.21	
DC418	15.83	1.21	−25.84	27.05		DC391	5.58	2.04			
DC417	15.08	1.53				DC390	5.23	2.40			
DC416	14.33	1.15				DC389	4.88	2.10	−24.72	26.82	
DC415	13.98	1.40	−25.93	27.33		DC388	4.62	2.00			*Crepida*
DC414	13.63	1.69				DC387	4.44	2.07			
DC413	13.28	1.60				DC386	4.25	2.19			
DC412	12.93	1.73	−25.95	27.68		DC385	4.07	2.29	−24.15	26.44	
DC411	12.58	1.86				DC383	3.55	2.34			
DC410	12.23	1.65				DC382	3.31	2.73			
DC378	2.40	2.75	−24.09	26.84		DC349	−0.94	1.30	−26.45	27.75	
DC377	2.07	3.03				DC348	−1.06	1.54			
DC376	2.03	2.57	−24.38	26.95		DC347	−1.18	1.22			
DC372	1.87	2.71				DC346	−1.30	0.84	−25.47	26.31	
DC371	1.77	2.71				DC345	−1.42	1.51			
DC369	1.49	2.51	−24.43	26.94		DC344	−1.49	0.59			
DC367	1.21	2.40				DC343	−1.56	1.63	−26.89	28.52	
DC366	1.07	2.53				DC342	−1.66	1.27			
DC365	0.95	2.32	−24.49	26.81		DC341	−1.76	1.65			
DC364	0.83	2.40				DC333	−2.24	1.31	−26.56	27.87	
DC363	0.63	2.05				DC331	−2.42	0.54			
DC362	0.50	2.39				DC330	−2.50	0.68	−26.22	26.90	
DC361	0.35	2.46				DC329	−2.59	0.76			
DC360	0.25	1.51	−24.43	25.94		DC328	−2.68	0.73			
DC359	0.15	0.86			*Triangularis*	DC327	−2.76	0.61	−27.76	28.37	
DC358	0.00	0.94	−25.22	26.16		DC326	−2.85	0.40			
DC357	−0.15	1.66	−25.12	26.78		DC325	−2.93	0.63			
DC356	−0.25	1.85				DC324	−3.02	0.54	−27.56	28.10	
DC355	−0.35	1.57	−25.52	27.09		DC323	−3.15	0.56			
DC354	−0.42	1.01				DC322	−3.28	0.80		28.24	
DC353	−0.54	1.38	−24.46	25.84		DC321	−3.41	0.70	−27.54		
DC352	−0.66	1.41				DC320	−3.54	0.60			
DC351	−0.74	0.82	−25.73	26.55		DC319	−3.67	0.62			
DC350	−0.82	1.68				DC318	−4.03	0.61	−28.12	28.73	
DC317	−4.39	0.71				DC291	−10.36	0.43			
DC316	−4.75	0.75	−27.95	28.70		DC290	−10.71	0.59			
DC315	−5.11	0.67				DC289	−11.06	0.29			
DC313	−5.83	0.60	−28.29	28.89		DC288	−11.41	0.04			
DC311	−6.55	0.83				DC286	−12.11	0.00	−27.94	27.94	
DC310	−6.91	0.47				DC285	−12.46	0.52			
DC309	−7.06	0.40	−27.94	28.34		DC284	−12.81	0.41			
DC308	−7.21	0.54				DC283	−13.16	0.50			
DC307	−7.36	0.42				DC282	−13.51	0.55			
DC306	−7.51	0.58				DC281	−13.86	0.40	−27.17	27.57	
DC305	−7.66	0.54				DC280	−14.21	0.29			
DC304	−7.81	0.41	−27.56	27.97		DC279	−14.56	0.11			
DC303	−7.96	0.55				DC278	−14.91	0.65	−27.50	28.15	
DC302	−8.11	0.53				DC277	−15.26	0.60			
DC301	−8.26	0.69				DC276	−15.61	0.50			
DC300	−8.41	1.06				DC275	−15.96	0.53	−25.79	26.32	
DC299	−8.56	0.53				DC274	−16.31	1.26			
DC298	−8.71	0.40				DC273	−16.66	1.61			*Linguiformis*
DC297	−8.86	0.43				DC272	−17.01	1.22	−24.36	25.58	
DC296	−9.01	0.14				DC270	−17.71	1.58			
DC295	−9.16	0.15	−27.70	27.85		DC265	−19.46	0.26	−24.98	25.24	
DC294	−9.31	0.21				DC263	−20.16	−0.50			
DC293	−9.66	0.41	−27.25	27.66		DC262	−20.51	−0.52	−25.31	24.79	
DC292	−10.01	0.60				DC261	−20.86	−0.63			

Table 1. (continued)

Code	Depth	$\delta^{13}C_{carb}$	$\delta^{13}C_{org}$	$\Delta^{13}C$	Fossil Age	Code	Depth	$\delta^{13}C_{carb}$	$\delta^{13}C_{org}$	$\Delta^{13}C$	Fossil Age
DC260	−21.21	−0.73	−28.02	27.29		DC234	−31.61	0.30	−28.78	29.08	
DC259	−21.56	−0.36				DC233	−33.11	0.10			
DC258	−21.91	−0.84	−28.75	27.91	*L. Rhenana*	DC232	−33.46	0.60			
DC257	−22.26	−0.35				DC231	−33.81	0.16			
DC256	−22.61	−0.14				DC230	−34.16	−0.10			
DC255	−22.96	−0.64				DC229	−34.51	0.20			
DC254	−23.31	−0.25				DC228	−34.86	0.10			
DC253	−23.66	−0.20				DC227	−35.21	1.07			
DC252	−24.01	−0.30				DC226	−35.56	0.30			
DC250	−24.36	−0.50	−28.31	27.81		DC225	−35.91	0.50			
DC249	−24.71	0.20				DC224	−36.26	0.02			
DC248	−25.06	0.50				DC223	−36.61	0.28			
DC247	−25.41	−0.02				DC222	−36.96	0.16	−28.65	28.81	
DC246	−25.76	0.10				DC221	−37.31	0.18			
DC245	−26.11	−0.30				DC220	−37.66	0.17			
DC244	−26.46	0.50	−28.69	29.19		DC219	−38.01	0.20			
DC243	−26.81	0.00									
DC242	−27.16	−0.30									
DC241	−27.51	−0.50									
DC240	−29.51	−0.30	−27.96	27.66							
DC239	−29.86	0.10									
DC238	−30.21	−0.10									
DC237	−30.56	0.20									
DC236	−30.91	0.00									
						Yangdi Section					
YT-001	−24.45	1.36	−26.36	27.72		YT-027	−19.25	1.44			
YT-002	−24.25	0.86				YT-028	−19.05	1.63			
YT-003	−24.05	0.43	−28.47	28.90		YT-029	−18.85	1.53			
YT-004	−23.85	2.77				YT-030	−18.65	1.60			
YT-005	−23.65	2.75	−24.31	27.06		YT-031	−18.45	1.65			
YT-006	−23.45	2.66				YT-032	−18.25	1.47	−28.42	29.89	
YT-007	−23.25	2.97	−25.81	28.78		YT-033	−18.05	1.30			
YT-008	−23.05	3.30				YT-034	−17.85	1.37			
YT-009	−22.85	2.81				YT-035	−17.65	1.32			
YT-010	−22.65	3.15				YT-036	−17.45	1.41			
YT-014	−21.85	2.36				YT-037	−17.25	1.13			
YT-015	−21.65	2.21	−25.34	27.55		YT-038	−17.05	1.18			
YT-016	−21.45	2.39				YT-039	−16.85	1.25			
YT-017	−21.25	2.11				YT-040	−16.65	1.31			
YT-018	−21.05	1.81				YT-041	−16.45	1.17	−26.89	28.06	
YT-019	−20.85	2.24				YT-042	−16.25	1.30			
YT-020	−20.65	1.24				YT-043	−16.05	0.85			
YT-021	−20.45	1.39	−27.94	29.33		YT-044	−15.85	0.80			
YT-022	−20.25	1.20				YT-045	−15.65	0.79			
YT-023	−20.05	1.35				YT-046	−15.45	0.75			
YT-024	−19.85	1.44				YT-047	−15.25	0.78			
YT-025	−19.65	1.27				YT-048	−15.05	0.96			
YT-026	−19.45	1.26				YT-049	−14.85	0.88			
YT-050	−14.65	0.96				YT-081	−8.45	0.66			*Rhenana*
YT-051	−14.45	0.89	−28.46	29.35		YT-082	−8.25	0.70			
YT-052	−14.25	0.68				YT-083	−8.05	0.76			
YT-053	−14.05	0.86				YT-084	−7.95	0.97			
YT-054	−13.85	0.87				YT-085	−7.85	0.45			
YT-055	−13.65	0.92				YT-086	−7.75	0.54	−28.33	28.87	
YT-057	−13.25	0.87				YT-087	−7.65	0.52			
YT-058	−13.05	0.75				YT-088	−7.55	0.72			
YT-059	−12.85	0.62				YT-089	−7.45	0.81			
YT-061	−12.45	0.35				YT-090	−7.35	0.81			
YT-063	−12.05	0.26				YT-091	−7.25	0.91			
YT-064	−11.85	0.37				YT-092	−7.15	0.79			
YT-065	−11.65	0.65				YT-093	−7.05	0.58			
YT-066	−11.45	0.61				YT-094	−6.95	0.56			
YT-067	−11.25	0.63				YT-095	−6.85	0.66			
YT-068	−11.05	0.59	−27.70	28.29		YT-096	−6.75	0.78			
YT-069	−10.85	0.66				YT-097	−6.65	0.66			
YT-070	−10.65	0.71				YT-098	−6.55	0.54			
YT-075	−9.65	0.81				YT-099	−6.45	0.63			
YT-076	−9.45	0.57				YT-100	−6.35	0.70			
YT-077	−9.25	0.59				YT-101	−6.25	0.66			
YT-078	−9.05	0.27				YT-102	−6.15	0.40			
YT-079	−8.85	0.47				YT-103	−6.05	0.24			

Table 1. (continued)

Code	Depth	$\delta^{13}C_{carb}$	$\delta^{13}C_{org}$	$\Delta^{13}C$	Fossil Age	Code	Depth	$\delta^{13}C_{carb}$	$\delta^{13}C_{org}$	$\Delta^{13}C$	Fossil Age
YT-080	−8.65	0.52				YT-104	−5.95	0.13			
YT-105	−5.85	0.64				YT-133	−3.05	0.35			
YT-106	−5.75	0.27	−28.13	28.40		YT-134	−2.95	0.33			
YT-107	−5.65	0.09				YT-135	−2.85	0.42			
YT-111	−5.25	0.74				YT-136	−2.75	0.4254	−26.21	26.64	
YT-112	−5.15	0.53				YT-137	−2.65	0.81			
YT-113	−5.05	0.44				YT-138	−2.55	0.45			
YT-114	−4.95	0.63				YT-139	−2.45	0.54			
YT-115	−4.85	0.52				YT-140	−2.35	0.49			
YT-116	−4.75	0.61				YT-141	−2.25	0.5236	−26.58	27.10	
YT-118	−4.55	0.71				YT-142	−2.15	1.04			
YT-119	−4.45	0.85				YT-143	−2.05	0.88			
YT-120	−4.35	0.86				YT-144	−1.95	0.51			
YT-121	−4.25	0.52				YT-145	−1.85	0.52			
YT-122	−4.15	0.64				YT-146	−1.75	0.6804	−26.56	27.24	
YT-123	−4.05	0.72				YT-147	−1.65	0.69			
YT-124	−3.95	0.79				YT-148	−1.55	0.69			
YT-125	−3.85	0.56				YT-149	−1.45	0.84	−26.77	27.61	
YT-126	−3.75	0.6718	−28.27	28.94		YT-150	−1.40	1.81			
YT-127	−3.65	0.26				YT-151	−1.35	2.43			
YT-128	−3.55	0.42				YT-152	−1.25	2.31			
YT-129	−3.45	0.53				YT-153	−1.15	1.64			
YT-130	−3.35	0.53				YT-154	−1.05	1.92			
YT-131	−3.25	0.5334	−27.56	28.09		YT-155	−0.95	2.03	−25.45	27.47	
YT-132	−3.15	0.36				YT-156	−0.85	1.9876			
YT-157	−0.75	2.13				YT-181	0.50	3.04			
YT-158	−0.65	1.68	−25.73	27.42		YT-182	0.55	3.46			
YT-159	−0.60	1.935				YT-183	0.60	2.96			
YT-160	−0.55	2.21				YT-184	0.70	2.76	−24.79	27.55	
YT-161	−0.50	2.56	−25.47	28.03		YT-185	0.80	2.4682			
YT-162	−0.45	2.1736				YT-186	0.90	2.01			
YT-163	−0.40	2.54				YT-187	1.00	2.01	−24.05	26.06	
YT-164	−0.35	2.44	−25.24	27.68		YT-188	1.10	2.23			
YT-165	−0.30	2.58				YT-189	1.20	2.08			
YT-166	−0.25	2.80				YT-190	1.30	2.12			
YT-167	−0.20	2.59	−25.51	28.10		YT-191	1.40	2.22			
YT-168	−0.15	2.4624	−25.71	28.18		YT-192	1.50	2.97	−24.12	27.09	
YT-169	−0.10	2.51	−25.68	28.19		YT-193	1.60	2.3548			
YT-170	−0.05	2.29	−25.22	27.51		YT-194	1.70	2.80			
YT-171	0.00	2.41			*Linguiformis*	YT-195	1.80	2.87			
YT-172	0.05	3.18			*Triangularis*	YT-196	1.90	2.73			
YT-173	0.10	2.98	−24.32	27.30		YT-197	2.00	2.70	−24.25	26.95	
YT-174	0.15	2.7778				YT-198	2.10	2.7896			
YT-175	0.20	3.13				YT-199	2.20	2.72			
YT-176	0.25	2.76	−24.55	27.31		YT-201	2.30	2.30			
YT-177	0.30	2.90				YT-202	2.50	2.66			
YT-178	0.35	3.57				YT-203	2.60	2.72			
YT-179	0.40	2.73	−25.41	28.13		YT-204	2.70	2.69			
YT-180	0.45	3.037				YT-205	2.80	2.52			
YT-206	2.90	2.65				YT-230	5.30	1.92			
YT-207	3.00	2.32	−24.59	26.91		YT-231	5.40	2.11			
YT-208	3.10	2.51				YT-232	5.50	2.12			
YT-209	3.20	2.63				YT-233	5.60	1.80			
YT-210	3.30	2.36				YT-234	5.70	1.98			
YT-211	3.40	2.42				YT-235	5.80	1.96			
YT-212	3.50	2.54				YT-236	5.90	2.07			
YT-213	3.60	2.38				YT-237	6.00	1.86			
YT-214	3.70	2.29				YT-238	6.10	1.86			
YT-215	3.80	2.26				YT-239	6.20	1.85			
YT-216	3.90	2.33				YT-240	6.30	1.79			
YT-217	4.00	2.30				YT-241	6.40	1.71			
YT-218	4.10	2.34				YT-242	6.50	1.86			
YT-219	4.20	2.03				YT-243	6.60	1.68			
YT-220	4.30	2.31				YT-244	6.70	1.73			
YT-221	4.40	2.26				YT-245	6.80	1.63			
YT-222	4.50	2.22				YT-246	6.90	1.52			
YT-223	4.60	2.10				YT-247	7.00	1.50	−26.20	27.70	
YT-224	4.70	2.14				YT-248	7.10	1.63			
YT-225	4.80	2.26				YT-249	7.20	1.44			
YT-226	4.90	2.24				YT-250	7.30	1.62			
YT-227	5.00	2.02	−25.46	27.48		YT-251	7.40	1.58			
YT-228	5.10	2.12				YT-252	7.50	1.55			

Table 1. (continued)

Code	Depth	$\delta^{13}C_{carb}$	$\delta^{13}C_{org}$	$\Delta^{13}C$	Fossil Age	Code	Depth	$\delta^{13}C_{carb}$	$\delta^{13}C_{org}$	$\Delta^{13}C$	Fossil Age
YT-229	5.20	1.91				YT-253	7.60	1.39			
YT-254	7.70	1.70									
YT-255	7.80	1.44									
YT-256	7.90	1.41									
YT-257	8.00	1.68									
YT-263	9.10	1.62									
YT-264	9.30	1.73									
YT-265	9.50	1.48									
YT-266	9.70	1.87									
YT-267	9.90	2.14									
YT-268	10.10	1.41									
YT-271	10.70	2.40	−26.33	28.73							
YT-272	10.90	1.32									
YT-273	11.10	2.08									
YT-274	11.30	1.99									

addition, the molecular isotope records [*Joachimski et al.*, 2002], which are believed to be less affected by diagenesis, do not show negative shifts during the period of $\delta^{13}C_{carb}$ increase. More importantly, the $\Delta^{13}C$ in the Fuhe section displays a decreasing trend at the F-F boundary, if the abnormal negative values of $\delta^{13}C_{carb}$ are discarded (Figure 3).

[13] Summarily, the carbon isotope records from south China (Dongcun, Yangdi, Fuhe) and Poland (Kowala, Psie Górki, Plucki, and Dębnik) show a similar pattern near the F-F boundary, which is characterized by a larger amplitude excursion of $\delta^{13}C_{org}$ than $\delta^{13}C_{carb}$, indicating that the decrease of $\Delta^{13}C$ might have a global significance.

[14] The larger amplitude shifts of $\delta^{13}C_{org}$ compared to $\delta^{13}C_{carb}$ and its resultant $\Delta^{13}C$ decrease could be caused by the changes of atmospheric CO_2 level [*Bidigare et al.*, 1997], and/or kinetic isotope effect from varying metabolic pathways, as well as the change in dominant sources of marine sedimentary organic matter, particularly the input of terrestrial organic matter [*Sackett and Thompson*, 1962; *Hinga et al.*, 1994; *Hayes et al.*, 1999; *Kienast et al.*, 2001].

[15] The input of terrestrial organic matter could not interpret the $\delta^{13}C_{org}$ shifts observed in this study. The Frasnian sequences of the Dongcun and Yangdi sections were deposited under different sedimentary environments [*Chen et al.*, 2001; *Wang and Ziegler*, 2002]. The Dongcun section was deposited under pelagic depositional condition, while the Yangdi section was deposited under a platform environment. Theoretically, the influx of terrestrial organic matter into the Yangdi section should be larger than that of the Dongcun section. Therefore, $\delta^{13}C_{org}$ values of the Yangdi section would be higher than those of the Dongcun section if the terrestrial organic matter were the dominant source of the sedimentary organic carbon, because the $\delta^{13}C$ of terrestrial organic materials is often higher than that of contemporaneous marine organics. However, the fact is that there are no observable differences in $\delta^{13}C_{org}$ between the

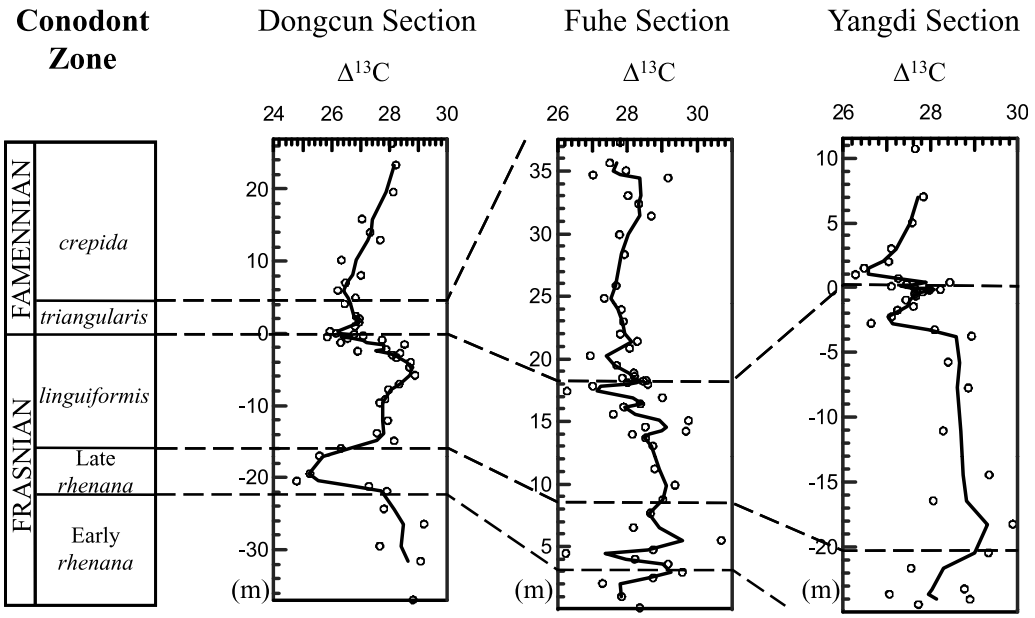

Figure 3. Variations of the $\Delta^{13}C$ in the Dongcun, Fuhe, and Yangdi sections (the data from the Fuhe section are adopted from *Chen et al.* [2005]). The solid line is the weighted average.

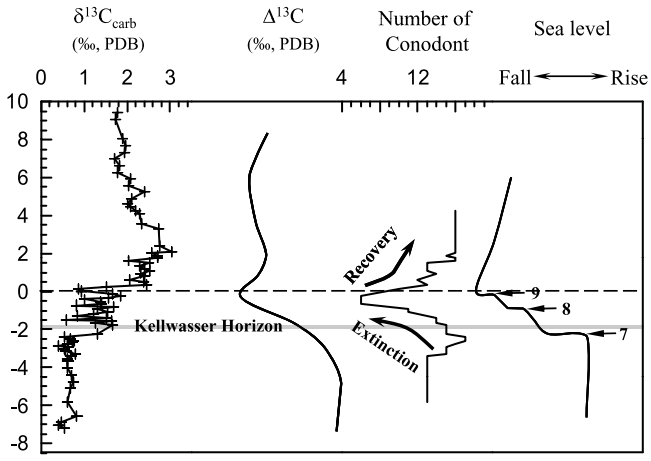

Figure 4. Relationships among $\delta^{13}C_{carb}$, $\Delta^{13}C$, conodont evolution, and sea level changes across the F-F boundary in the Dongcun section. The patterns of conodont evolution and sea level changes are comparable with the records from other continents and have a global signification. The numbers represent the events identified by *Sandberg et al.* [2002].

Dongcun and Yangdi sections. Furthermore, the maximum values of $\delta^{13}C_{org}$ in the Dongcun (−24.08‰) and Yangdi sections (−24.05‰) are larger than that of the Devonian terrestrial organic matter (−24.8‰ to −26.8‰) [*Maynard*, 1981]. The low $\delta^{13}C_{org}$ of terrestrial organic matter can hardly explain the larger $\delta^{13}C_{org}$ values near the F-F boundary.

[16] Though changes in metabolic pathway biomass community and growth rate have a potential for causing $\delta^{13}C_{org}$ shifts, carbon isotope analysis of total organic matter has been shown to faithfully record the original isotopic trend when compared with compound specific $\delta^{13}C_{org}$ analysis of short-chain n-alkanes as well as acyclic isoprenoids pristane, phytane, and hopane from identical samples [*Joachimski et al.*, 2002]. The baseline values of the different biomarkers varied by a few per mille but the trends shown were practically identical, suggesting that $\Delta^{13}C$ changes cannot be explained by variation in metabolic pathway and biomass community [*Cramer and Saltzman*, 2007]. Increased growth rate of the phytoplankton can also cause positive excursions of $\delta^{13}C_{org}$. The increased growth rate often increases primary productivities, leading to high influx of organic matter into sediments. The previous analysis on the Dongcun section showed that the carbon isotope shifts around the F-F boundary mainly resulted from the development of reducing conditions (Figure 2) [*Xu et al.*, 2008]. Therefore, the concentrations of organic matter would increase at the F-F boundary if the growth rate were the major factor for $\delta^{13}C_{org}$ shifts, because both reducing conditions and increased productivity favor for organic matter burial. However, there is no significant changes in organic matter contents during the interval with $\delta^{13}C_{org}$ shifts (Figure 2), suggesting changes in growth rate should not the major cause for the $\delta^{13}C_{org}$ changes. In addition, a study of a model versus measurement also indicates that the concentrations of dissolved CO_2 play a major role in the changes of $\delta^{13}C_{org}$, though growth rate and/or other biotic factors might cause some of the shifts in $\delta^{13}C_{org}$ [*Rau et al.*, 1997].

[17] Most important, the large amplitude excursion of $\delta^{13}C_{org}$ and its resulting $\Delta^{13}C$ decrease are considered to be the two typical characteristics of the carbon isotope variations caused by lowering pCO_2 level [*Popp et al.*, 1989; *Freeman and Hayes*, 1992; *Hayes et al.*, 1999]. The isotopic fractionation of ^{13}C during photosynthesis is a function of extracellular and intracellular CO_2 concentrations [*Popp et al.*, 1989; *Freeman and Hayes*, 1992; *Hayes et al.*, 1999; *Pagani et al.*, 1999] and the photosynthetic fractionation factor is negatively correlated with atmospheric CO_2 level [*Popp et al.*, 1989]. As a result, $\delta^{13}C_{org}$ would display a larger amplitude excursion than $\delta^{13}C_{carb}$ with decreasing atmospheric CO_2 level, and thus $\Delta\delta^{13}C$ shifts to negative.

[18] Consequently, the decrease of $\Delta^{13}C$ caused by larger amplitude of $\delta^{13}C_{org}$ than $\delta^{13}C_{carb}$ should mainly reflect the changes of atmospheric CO_2 level rather than the variations of metabolic pathways and/or dominant organic matter sources.

4.2. Associations of Carbon Cycle Change With Mass Extinction

[19] As reviewed by *Sandberg et al.* [2002], the F-F mass extinction had a close association with sea level changes. A stepwise extinction began with the severe sea level fall and the ultimate mass extinction took place well during severe eustatic falls that immediately followed major eustatic rises. These rapid changes of sea level are documented not only at the Steinbruch Schmidt section in a deep water, submarine-rise setting in Germany, but also at sections in inner shelf and outer shelf and slope settings in Belgium, Nevada, Utah [*Sandberg et al.*, 2002]. This evidence, together with the worldwide positive $\delta^{13}C_{carb}$ excursion, suggests that the F-F mass extinction might be associated with both the sea level and global carbon cycle changes.

[20] The detail eustatic changes and conodont evolution across the F-F boundary were reconstructed based on the records from the Dongcun section [*Wang and Ziegler*, 2002]. The sea level curve drawn based on the integrated analysis of biofacies, lithofacies, and sequence stratigraphy in the Dongcun section [*Wang and Ziegler*, 2002] is comparable with the most widely accepted sea level curve produced by *Sandberg et al.* [2002], further supporting that the records in the Dongcun section have a global signification. These data, together with the carbon isotope records, make it possible for scrutinizing the associations of the carbon cycle changes with biomass extinction through analyzing the phase differences among the global carbon cycle change, sea level change, and conodont extinctions.

[21] The conodont extinction displays a close association with the eustatic changes around the F-F boundary in the Dongcun section [*Wang and Ziegler*, 2002] (Figure 4). In the early *linguiformis* zone, *Palmatolepis*, a pelagic genus which favored the farthest offshore and deep water setting [*Sandberg and Ziegler*, 1996], is dominant with an average more than 85% of total fauna, indicating a typical palmatolepid biofacies. Based on the analysis of sequence stratigraphy, this interval is a highstand systems tract, corresponding to the upper part of eustatic rise Event 5 of *Sandberg et al.* [2002] [*Wang and Ziegler*, 2002]. Then the "Upper KW Horizon" (−2.04 to −1.84 m) event suddenly happened, the facies instantaneously changed into dark limestone, indicating the beginning of remarkable sea level fall (Figure 4). A thick-bedded shallow water limestone developed from −2.0 to 0 m.

The fauna in this interval is a typical reduced or impoverished in Frasnian fauna. Conodonts are low in diversities, scarce in number of individuals, and all are surviving taxa from the underlying sequence. The deposition from −2.0 to −0.8 m corresponds to Event 7 of *Sandberg et al.* [2002] (Figure 4). The final extinction of *Palmatolepis linguiformis* is at –0.82 m, corresponding to the beginning of the more rapid shallowing (Event 8 of *Sandberg et al.* [2002]) (Figure 4). The stratum of −0.4 to 0 m is an important interval of sea level changes, indicating the most pronounced shallowing facies. No conodonts have been found at the F-F boundary; this interval could actually be a big extinction, corresponding to Event 9 of *Sandberg et al.* [2002] (Figure 4). From the base of the *triangularis* zone, the strata thin upward and consist of dark thin-bedded limestones, representing a relatively rapid sea level rise (Figure 4). From the late *triangularis* zone to the early *crepida* zone, the facies changes into deeper water, but is still much shallower than the depositional facies below −1.98 m [*Wang and Ziegler*, 2002].

[22] The direct effect of marine regression is reducing the habitat areas on continental shelves for shallow marine species. However, this assumption can hardly explain species loss of terrestrial ecosystem because the areal extent and habitat of the terrestrial realm should increase with the marine regression [*Boulter et al.*, 1988; *Raymond and Metz*, 1992, 1995] In addition, *Jablonski* [1986] suggested that only 13% of modern families would become extinct even if all the modern shelf biota were eliminated. Thus, the sea level fall alone could not cause the F-F mass extinction.

[23] Figure 4 shows the associations of conodonts extinction with the carbon cycle, eustatic change, and the detailed evolution of condonts across the F-F boundary in the Dongcun section. The onset of eustatic fall postdates the beginnings of $\delta^{13}C_{carb}$ and $\Delta^{13}C$ shift, and the largest marine regression occurs during the interval with lowest $\Delta^{13}C$ values (Figure 4). These characteristics provide key evidence for interpreting the relationship between sea level change and increased organic carbon burials. The increased organic carbon burial can lead to decrease in atmospheric CO_2 level [*Kump and Arthur*, 1999], which is commonly taken to be the main driver of climate change on geological timescales [*Berner and Kothavala*, 2001; *Royer et al.*, 2004]. The lower pCO_2 would lead to temperature decrease through weakening greenhouse effect. With temperature decrease, an ice cap would develop in high altitude and latitude, causing sea level fall. This postulation is supported by the temperature decrease indicated by the $\delta^{18}O$ of conodont apatite across the F-F boundary [*Joachimski and Buggisch*, 2002]. Significant temperature decline would decimate reefal and tropical ecosystems, as species inhabiting these places have no refuge against cold. In contrast, the high-latitude species could migrate to lower latitudes and maintain their tolerable temperature. Each of these expected patterns of ecological selectivity in survival are observed in the F-F event [*McGhee*, 1996], suggesting that the temperature decline should be an important factor for the mass extinction.

[24] For the causes of the increased carbon burial around the F-F boundary, our previous high-resolution investigations [*Xu et al.*, 2008] revealed that the reducing conditions predate the onset of the carbon isotope excursions, suggesting that the two positive carbon isotope shifts are likely caused by the expansion of anoxic conditions. The low Al/(Al+Fe) ratio across the F-F boundary leads the U/Al and Cu/Al anomalies in timing, implying that this anoxic event might have resulted from a long-term cumulative effect of intense hydrothermal-volcanic activities. Therefore, long-term cumulative effect of intense hydrothermal-volcanic activities lead to development and expansion of anoxic water mass, which in turn cause increased organic carbon burial and thus atmospheric CO_2 level decrease.

[25] In the late *rhenana* zone, a positive $\delta^{13}C_{carb}$ excursion has been detected on the worldwide. This positive excursion, together with organic rich sediments (lower Kellwasser horizon), indicates another perturbation of global carbon cycle in the late *rhenana* zone. However, no obvious positive shift of $\delta^{13}C_{org}$ has been detected in the late *rhenana* zone in most previous studies. *Joachimski et al.* [2002] suggest the $\delta^{13}C_{org}$ maximum might be missed due to the broader sampling interval. The carbon isotope records in the Dongcun and Yangdi sections provide critical evidence for the above postulation. The carbon isotope records in the Dongcun and Fuhe sections display a similar pattern in the late *rhenana* zone with that at the F-F boundary, which is characterized by a relatively larger positive shift in $\delta^{13}C_{org}$ than $\delta^{13}C_{carb}$ (Figure 2) and negative $\Delta^{13}C$ shift (Figure 3). These characteristics suggest that a perturbation of carbon cycle like that at the F-F boundary might occur in the late *rhenana* zone.

5. Conclusions

[26] The negative $\Delta^{13}C$ shifts and the larger amplitude shift of $\delta^{13}C_{org}$ positive excursion than $\delta^{13}C_{carb}$ document the decreases in pCO_2 level with increased organic carbon burial in the late *rhenana* zone and at the F-F boundary. The timing of carbon isotope excursions, eustatic change, and conodont evolution across the F-F boundary provides key evidence for identifying the association of carbon cycle with the mass extinction. The onset of conodonts extinction coincides with the sea level fall, while it postdates that of atmospheric CO_2 level decrease. Furthermore, the severest extinction occurs during the interval with the lowest pCO_2 level and sea level. These observations suggest that the environmental changes induced by lowering pCO_2 level, such as temperature decrease and marine regression, might be the important factors for the F-F mass extinction.

[27] **Acknowledgments.** We gratefully acknowledge Zhang Fusong and Wen Chuanfen's help for stable isotope analyses and the assistance of Lu Hongjin and Li Zhenliang for field work. Special acknowledgment is owed to Grzegorz Racki and two anonymous reviewers for their critical advice and suggestions. This work is funded by National Natural Science Foundation (40972227) and the Major State Basic Research Development Program of China (973 Program) (2010CB950203).

References

Allan, J. R., and R. K. Matthews (1982), Isotope signatures associated with early meteoric diagenesis, *Sedimentology*, *29*, 797–817, doi:10.1111/j.1365-3091.1982.tb00085.x.

Bambach, R. K., A. H. Knoll, and S. C. Wang (2004), Origination extinction and mass depletions of marine diversity, *Paleobiology*, *30*, 522–542, doi:10.1666/0094-8373(2004)030<0522:OEAMDO>2.0.CO;2.

Banner, J. L., and G. N. Hanson (1990), Calculation of simultaneous isotopic and trace element variations during water-rock interaction with applications to carbonate diagenesis, *Geochim. Cosmochim. Acta*, *54*, 3123–3137, doi:10.1016/0016-7037(90)90128-8.

Berner, R. A., and Z. Kothavala (2001), GEOCARB III: A revised model of atmospheric CO_2 over Phanerozoic time, *Am. J. Sci.*, *301*, 182–204, doi:10.2475/ajs.301.2.182.

Bidigare, R. R., et al. (1997), Consistent fractionation of ^{13}C in nature and in the laboratory: Growth rate effects in some haptophyte algae, *Global Biogeochem. Cycles*, *11*, 279–292, doi:10.1029/96GB03939.

Boulter, M. C., R. A. Spicer, and B. A. Thomas (1988), Patterns of plants extinction from some palaeobotanical evidence, in *Extinction and Survival in the Fossil Record*, *Syst. Assoc. Spec. Vol.*, vol. 34, edited by G. P. Larwood, pp. 1–36, Clarendon, New York.

Buggisch, W., and M. M. Joachimski (2006), Carbon isotope stratigraphy of the Devonian of central and southern Europe, *Palaeogeogr. Palaeoclimatol. Palaeoecol.*, *240*, 68–88, doi:10.1016/j.palaeo.2006.03.046.

Chen, D., M. E. Tucker, J. Zhu, and M. Jiang (2001), Carbonate sedimentation in a starved pull-apart basin, Middle to Late Devonian, southern Guilin, south China, *Basin Res.*, *13*, 141–167, doi:10.1046/j.1365-2117.2001.00148.x.

Chen, D., H. Qing, and R. Li (2005), The Late Devonian Frasnian-Famennian (F/F) biotic crisis: Insights from $\delta^{13}C_{carb}$, $\delta^{13}C_{org}$ and $^{87}Sr/^{86}Sr$ isotopic systematics, *Earth Planet. Sci. Lett.*, *235*, 151–166, doi:10.1016/j.epsl.2005.03.018.

Cramer, B. D., and M. R. Saltzman (2007), Early Silurian paired $\delta^{13}C_{carb}$ and $\delta^{13}C_{org}$ analyses from the midcontinent of North America: Implications for paleoceanography and paleoclimate, *Palaeogeogr. Palaeoclimatol. Palaeoecol.*, *256*, 195–203, doi:10.1016/j.palaeo.2007.02.032.

Des Marais, D. J. (2001), Isotopic evolution of the biochemical carbon cycle during the Precambrian, *Rev. Mineral. Geochem.*, *43*, 555–578, doi:10.2138/gsrmg.43.1.555.

Fischer, G., P. J. Müller, and G. Wefer (1998), Latitudinal $\delta^{13}C_{org}$ variations in sinking matter and sediments from the South Atlantic: Effects of anthropogenic CO_2 and implications for paleo-pCO_2 reconstructions, *J. Mar. Syst.*, *17*, 471–495, doi:10.1016/S0924-7963(98)00059-1.

Francois, R., M. A. Altabet, R. Goericke, D. C. McCorkle, C. Brunet, and A. Poisson (1993), Changes in the $\delta^{13}C$ of surface water particulate organic matter across the subtropical convergence in the SW Indian Ocean, *Global Biogeochem. Cycles*, *7*, 627–644, doi:10.1029/93GB01277.

Freeman, K. H., and J. M. Hayes (1992), Fractionation of carbon isotopes by phytoplankton and estimates of ancient pCO_2 levels, *Global Biogeochem. Cycles*, *6*, 185–189, doi:10.1029/92GB00190.

Goddéris, Y., and M. M. Joachimski (2004), Global change in the Late Devonian: Modelling the Frasnian-Famennian short-term carbon isotope excursions, *Palaeogeogr. Palaeoclimatol. Palaeoecol.*, *202*, 309–329, doi:10.1016/S0031-0182(03)00641-2.

Gong, C., and D. J. Hollander (1997), Differential contribution of bacteria to sedimentary organic matter in oxic and anoxic environments, Santa Monica Basin, California, *Org. Geochem.*, *26*, 545–563, doi:10.1016/S0146-6380(97)00018-1.

Hayes, J. M., B. N. Popp, R. Takigiku, and M. W. Johnson (1989), An isotopic study of biogeochemical relationships between carbonate and organic carbon in the Greenhorn Formation, *Geochim. Cosmochim. Acta*, *53*, 2961–2972, doi:10.1016/0016-7037(89)90172-5.

Hayes, J. M., H. Strauss, and A. J. Kaufman (1999), The abundance of ^{13}C in marine organic matter and isotopic fractionation in the global biogeochemical cycle of carbon during the past 800 Ma, *Chem. Geol.*, *161*, 103–125, doi:10.1016/S0009-2541(99)00083-2.

Hinga, K. R., M. A. Arthur, M. E. Q. Pilson, and D. Whitaker (1994), Carbon isotope fractionation by marine phytoplankton in culture: The effects of CO_2 concentration, pH, temperature, and species, *Global Biogeochem. Cycles*, *8*, 91–102, doi:10.1029/93GB03393.

Izokh, O. P., N. G. Izokh, V. A. Ponomarchuk, and D. V. Semenova (2009), Carbon and oxygen isotopes in the Frasnian-Famennian section of the Kuznetsk basin (southern West Siberia), *Russ. Geol. Geophys.*, *50*, 610–617, doi:10.1016/j.rgg.2008.12.007.

Jablonski, D. (1986), Causes and consequences of mass extinctions: A comparative approach, in *Dynamics of Extinction*, edited by D. K. Elliott, pp. 183–229, John Wiley, New York.

Ji, Q. (1994), On the Frasnian-Famennian extinction event in south China as viewed in the light of conodont study [in Chinese with English abstract], *Prof. Pap. Strat. Palaeontol.*, *24*, 79–107.

Joachimski, M. M. (1997), Comparison of organic and inorganic carbon isotope patterns across the Frasnian-Famennian boundary, *Palaeogeogr. Palaeoclimatol. Palaeoecol.*, *132*, 133–145, doi:10.1016/S0031-0182(97)00051-5.

Joachimski, M. M., and W. Buggisch (1993), Anoxic event in the late Frasnian—Causes of the Frasnian-Famennian faunal crisis?, *Geology*, *21*, 675–678, doi:10.1130/0091-7613(1993)021<0675:AEITLF>2.3.CO;2.

Joachimski, M. M., and W. Buggisch (2002), Conodont apatite delta signatures indicate climatic cooling as a trigger of the Late Devonian (F-F) mass extinction, *Geology*, *30*, 711–714, doi:10.1130/0091-7613(2002)030<0711:CAOSIC>2.0.CO;2.

Joachimski, M. M., R. D. Pancost, K. H. Freeman, C. Ostertag-Henning, and W. Buggisch (2002), Carbon isotope geochemistry of the Frasnian-Famennian transition, *Palaeogeogr. Palaeoclimatol. Palaeoecol.*, *181*, 91–109, doi:10.1016/S0031-0182(01)00474-6.

John, E. H., P. B. Wignall, R. J. Newton, and S. H. Bottrell (2010), $\delta^{34}S_{CAS}$ and $\delta^{18}O_{CAS}$ records during the Frasnian-Famennian (Late Devonian) transition and their bearing on mass extinction models, *Chem. Geol.*, *275*, 221–234, doi:10.1016/j.chemgeo.2010.05.012.

Kienast, M., S. E. Calvert, C. Pelejero, and J. O. Grimalt (2001), A critical review of marine sedimentary $\delta^{13}C_{org}$-pCO_2 estimates: New palaeorecords from the South China Sea and a revisit of other low-latitude $\delta^{13}C_{org}$-pCO_2 records, *Global Biogeochem. Cycles*, *15*, 113–127, doi:10.1029/2000GB001285.

Kump, L. R., and M. A. Arthur (1999), Interpreting carbon-isotope excursions: Carbonate and organic matter, *Chem. Geol.*, *161*, 181–198, doi:10.1016/S0009-2541(99)00086-8.

Laws, E. A., R. R. Bidiggare, and B. N. Popp (1997), Effect of growth rate and CO_2 concentration on carbon isotopic fractionation by the marine diatom *Phaeodactylum tricornutum*, *Limnol. Oceanogr.*, *42*, 1552–1560, doi:10.4319/lo.1997.42.7.1552.

Lohmann, K. C. (1988), Geochemical patterns of meteoric diagenetic systems and their application to studies to palaeokarst, in *Palaeokarst*, edited by N. P. James and P. W. Choquette, pp. 58–80, Springer, Berlin, doi:10.1007/978-1-4612-3748-8_3.

Ma, X. P., and S. L. Bai (2002), Biological, depositional, microspherule, and geochemical records of the Frasnian–Famennian boundary beds, south China, *Palaeogeogr. Palaeoclimatol. Palaeoecol.*, *181*, 325–346, doi:10.1016/S0031-0182(01)00484-9.

Marshall, J. D. (1992), Climatic and oceanographic isotopic signals from the carbonate rock record and their preservation, *Geol. Mag.*, *129*, 143–160, doi:10.1017/S0016756800008244.

Maynard, J. B. (1981), Carbon isotopes as indicators of dispersal patterns in the Devonian-Mississippian shales of the Appalachian Basin, *Geology*, *9*, 262–265, doi:10.1130/0091-7613(1981)9<262:CIAIOD>2.0.CO;2.

McGhee, G. R. (1996), *The Late Devonian Mass Extinction*, Columbia Univ. Press, New York.

McGhee, G. R., L. J. Orth, L. R. Quitana, J. S. Gilmore, and E. J. Olsen (1986), Late Devonian "Kellwasser Event" mass-extinction horizon in Germany: No chemical evidence for a large body impact, *Geology*, *14*, 776–779, doi:10.1130/0091-7613(1986)14<776:LDKEMH>2.0.CO;2.

Pagani, M., M. A. Arthur, and K. H. Freeman (1999), Miocene evolution of atmospheric carbon dioxide, *Paleoceanography*, *14*, 273–292, doi:10.1029/1999PA900006.

Panchuk, K. M., C. Holmden, and S. A. Leslie (2006), Local controls on carbon cycling in the Ordovician midcontinent region of North America, with implications for carbon isotope secular curves, *J. Sediment. Res.*, *76*, 200–211, doi:10.2110/jsr.2006.017.

Popp, B. N., R. Takigiku, J. M. Hayes, J. W. Louda, and E. W. Baker (1989), The post-Paleozoic chronology and mechanism of ^{13}C depletion in primary marine organic matter, *Am. J. Sci.*, *289*, 436–454, doi:10.2475/ajs.289.4.436.

Racki, G. (2005), Toward understanding Late Devonian global events: Few answers, many questions, *Dev. Palaeontol. Stratigr.*, *20*, 5–36, doi:10.1016/S0920-5446(05)80002-0.

Racki, G., M. Racka, H. Matyja, and X. Devleeschouwer (2002), The Frasnian/Famennian boundary interval in the South Polish-Moravian shelf basins: Integrated event-stratigraphical approach, *Palaeogeogr. Palaeoclimatol. Palaeoecol.*, *181*, 251–297, doi:10.1016/S0031-0182(01)00481-3.

Rau, G., U. Riebesell, and D. Worlf-Gladrow (1997), CO2aq-dependent photosynthetic 13C fractionation in the ocean: A model versus measurements, *Global Biogeochem. Cycles*, *11*, 267–278, doi:10.1029/97GB00328.

Raymond, A., and C. Metz (1992), Land plants and the Frasnian-Famennian extinction event, *Geol. Soc. Am. Abstr. Programs*, *24*, Abstract A271.

Raymond, A., and C. Metz (1995), Laurussian land-plant diversity during the Silurian and Devonian: Mass extinction, sampling bias, or both?, *Paleobiology*, *21*, 74–91.

Riquier, L., N. Tribovillard, O. Averbuch, X. Devleeschouwer, and A. Riboulleau (2006), The late Frasnian Kellwasser horizons of the Harz Mountains (Germany): Two oxygen-deficient periods resulting from different mechanisms, *Chem. Geol.*, *233*, 137–155, doi:10.1016/j.chemgeo.2006.02.021.

Rosales, I., S. Quesada, and S. Robles (2001), Primary and diagenetic isotopic signals in fossils and hemipelagic carbonates: The Lower Jurassic of northern Spain, *Sedimentology*, *48*, 1149–1169, doi:10.1046/j.1365-3091.2001.00412.x.

Royer, D. L., R. A. Berner, I. P. Montañez, N. J. Tabor, and D. J. Beerling (2004), CO_2 as a primary driver of Phanerozoic climate, *GSA Today*, *14*, 4–10, doi:10.1130/1052-5173(2004)014<4:CAAPDO>2.0.CO;2.

Sackett, W. M., and R. R. Thompson (1962), Stable carbon isotopes in organic material in Upper Gulf of Mexico and near-by continental sediments, *Spec. Pap. Geol. Soc. Am.*, *47*, 258–259.

Saltzman, M. R. (2002), Carbon isotope ($\delta^{13}C$) stratigraphy across the Silurian-Devonian transition in North America: Evidence for a perturbation of the global carbon cycle, *Palaeogeogr. Palaeoclimatol. Palaeoecol.*, *187*, 83–100, doi:10.1016/S0031-0182(02)00510-2.

Sandberg, C. A., and W. Ziegler (1996), Devonian conodont biochronology in geologic time calibration, *Palaeobiodiversity Palaeoenviron.*, *76*, 259–265.

Sandberg, C. A., J. R. Morrow, and W. Ziegler (2002), Late Devonian sea-level changes, catastrophic events, and mass extinctions, in *Catastrophic Events and Mass Extinctions: Impacts and Beyond*, edited by C. Koeberl and K. G. MacLeod, *Geol. Soc. Am. Spec. Pap.*, *356*, 473–487.

Schindler, E. (1990), The late Frasnian (Upper Devonian) Kellwasser crisis, in *Extinction Events in Earth History, Proceedings of Project 216, Global Biological Events in Earth History*, *Lecture Notes Earth Sci.*, vol. 30, edited by E. G. Kauffman and O. H. Walliser, pp. 150–159, Springer, Berlin.

Stigall, A. L. (2010), Invasive species and biodiversity crises: Testing the link in the Late Devonian, *PLoS One*, *5*, e15584, doi:10.1371/journal.pone.0015584.

van Geldern, R., M. M. Joachimski, J. Day, U. Jansen, F. Alvarez, E. A. Yolkin, and X. P. Ma (2006), Carbon, oxygen and strontium isotope records of Devonian brachiopod shell calcite, *Palaeogeogr. Palaeoclimatol. Palaeoecol.*, *240*, 47–67, doi:10.1016/j.palaeo.2006.03.045.

Walliser, O. H. (1996), Global events in the Devonian and Carboniferous, in *Global Events and Event Stratigraphy*, edited by O. H. Walliser, pp. 225–250, Springer, Berlin, doi:10.1007/978-3-642-79634-0_11.

Wang, C. Y. (1994), Application of the Frasnian standard conodont zonation in south China, *Curr. Forschungsinst. Senchenberg*, *168*, 83–129.

Wang, C. Y., and W. Ziegler (2002), The Frasnian-Famennian conodont mass extinction and recovery in south China, *Senckenbergiana Lethaea*, *82*, 463–494, doi:10.1007/BF03042948.

Wang, K., H. H. J. Geldsetzer, W. D. Goodfellow, and H. R. Krouse (1996), Carbon and sulfur isotope anomalies across the Frasnian-Famennian extinction boundary, Alberta, Canada, *Geology*, *24*, 187–191, doi:10.1130/0091-7613(1996)024<0187:CASIAA>2.3.CO;2.

Xu, B., Z. Y. Gu, Q. Liu, C. Y. Wang, and Z. L. Li (2003), Carbon isotopic record from Upper Devonian carbonates at Dongcun in Guilin, south China, supporting the world-wide pattern of carbon isotope excursions during Frasnian-Famennian transition, *Chin. Sci. Bull.*, *48*, 1259–1264, doi:10.1360/02wd0474.

Xu, B., Z. Y. Gu, J. T. Han, and C. Y. Wang (2008), Environmental changes during Frasnian-Famennian transition in south China: A multiproxy approach, *J. Geophys. Res.*, *113*, G04033, doi:10.1029/2007JG000450.

Young, S. A., M. R. Saltzman, S. M. Bergström, S. A. Leslie, and X. Chen (2008), Paired $\delta^{13}C_{carb}$ and $\delta^{13}C_{org}$ records of Upper Ordovician (Sandbian-Katian) carbonates in North America and China: Implications for paleoceanographic change, *Palaeogeogr. Palaeoclimatol. Palaeoecol.*, *270*, 166–178, doi:10.1016/j.palaeo.2008.09.006.

Zeng, J. W., R. Xu, and Y. M. Gong (2011), Hydrothermal activities and seawater acidification in the Late Devonian F-F transition: Evidence from geochemistry of rare earth elements, *Sci. China, Ser. D Earth Sci.*, *54*, 540–549, doi:10.1007/s11430-011-4171-8.

Z. Gu, J. Han, Q. Hao, Q. Liu, Y. Lu, L. Wang, and B. Xu, Key Laboratory of Cenozoic Geology and Environment, Institute of Geology and Geophysics, Chinese Academy of Sciences, 19 Beitucheng West Rd., Beijing 100029, China. (bingx@mail.igcas.ac.cn)

C. Wang, Nanjing Institute of Geology and Palaeontology, Chinese Academy of Sciences, 30 East Beijing Rd., Nanjing 210008, China.